[3]A. Barbaro-Galtieri *et al.*, Rev. Mod. Phys. 42, 87 (1970). See especially p. 194.
[4]Seisaku Matsuda and S. Oneda, Phys. Rev. 174, 1992 (1968); Nucl. Phys. B9, 55 (1969). For a recent review, see S. Oneda and Seisaku Matsuda, *ibid.* B26, 203 (1971).
[5]S. Oneda, H. Umezawa, and S. Matsuda, Phys. Rev. Letters 25, 71 (1970).
[6]S. Oneda and Seisaku Matsuda, Phys. Rev. D 2, 324 (1970).
[7]We take in this paper $\eta'^0(958)$ as the $I=Y=0$ unitary singlet.
[8]S. Coleman and S. L. Glashow, Phys. Rev. Letters 6, 423 (1963); Phys. Rev. 134, B671 (1964).
[9]S. Okubo and B. Sakita, Phys. Rev. Letters 11, 50 (1963).
[10]S. Oneda and H. Yabuki, Phys. Rev. D 3, 2743 (1971).
[11]See, for example, R. E. Marshak, Riazuddin, and C. P. Ryan, *Theory of Weak Interactions in Particle Physics* (Wiley-Interscience, New York, 1969).
[12]Roughly speaking, an electromagnetic final-state interaction will be an additive effect to the one considered in this paper. It could change the values of $R_e \simeq R_\mu$ obtained to, for example, 0.96.
[13]Experimentally, the value of λ_+ is still controversial. It seems to vary from 0.02 to 0.05 depending on experiments.
[14]N. Brene, M. Roos, and A. Sirlin, Nucl. Phys. B6, 255 (1968).
[15]We note that our asymptotic symmetry predicts $g_+(0)=1$ to a good accuracy. Therefore, our asymptotic symmetry seems to be strongly supported by the present experiment.
[16]Note that in Ref. 9, where the existence of η' is not considered, the value of β is smaller, i.e., $\beta \simeq 0.0082$.
[17]S. Matsuda, S. Oneda, and P. Desai, Phys. Rev. 178, 2129 (1969).

PHYSICAL REVIEW D VOLUME 4, NUMBER 5 1 SEPTEMBER 1971

Electroproduction of Nucleon Resonances in a Relativistic Quark Model*

F. Ravndal
California Institute of Technology, Pasadena, California 91109
(Received 22 March 1971)

A relativistic version of the symmetric quark model is used to calculate the inelastic electron-proton scattering amplitudes in the resonance region. Including all the nucleon states of the harmonic-oscillator baryon spectrum, we find good agreement with the three prominent peaks in the cross section. The part of the cross section coming from longitudinally polarized virtual photons is small, as recently observed in the resonance region.

I. INTRODUCTION

One of the most promising fields of experimental high-energy physics during the last few years has turned out to be the inelastic scattering of electrons off protons and neutrons.[1] By observing only the final electron, one has the possibility of obtaining detailed information about the internal structure of the nucleons. One may hope this will have the same important consequences as the similar experiments of Franck and Hertz had for the understanding of atomic structure.

If one plots the measured cross section at a fixed scattering angle as a function of the energy E' of the final electron as in Fig. 1, the salient features of the data are the following:

(a) At low energy transfer to the nucleon, a few prominent bumps in the cross section, dying rapidly away with increasing incident electron energy (increasing momentum transfer);

(b) at large energy transfers, the domination of a continuous background which varies slowly with increasing momentum transfer.

At zero momentum transfer the inelastic electron scattering gives the total absorption cross section for real photons. In this case we know that the bumps are due to nucleon resonances. The continuous part will then correspond to what is called "Pomeranchuk exchange" in Regge language.

At the present time we have almost no real theoretical understanding of this latter part of the cross section. On the other hand, since the introduction of the quark model,[2] considerable insight has been gained into the classification and interactions of baryons and their resonances.

In this paper we will investigate electroproduction of nucleon resonances in the framework of the symmetric quark model picturing the baryon as a system of three quarks bound together by harmonic forces. This reaction being a highly relativistic process, there is little reason to believe that a nonrelativistic formulation of the quark model should be successful. As shown by Thornber,[3] the agreement with experiment is really not impressive and the longitudinal part of the cross section is too large compared to the transverse part. Be-

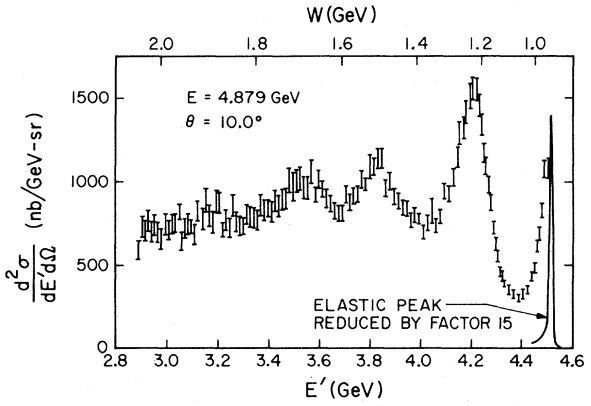

FIG. 1. Inelastic electron-proton cross sections at $E = 4.879$ GeV and $\theta = 10^0$ from Ref. 1.

sides being nonrelativistic, this version of the model also suffers from the necessity of expanding matrix elements in terms of the inverse of the nonphysical quark mass.

Recently, a relativistic formulation of the same model with no explicit quark mass has been developed by Feynman, Kislinger, and Ravndal.[4] The photoproduction amplitudes calculated from this model differ little from the nonrelativistic results[5] which agree generally well with experiment.[6] The only serious disagreement is found for the nucleon recurrence $F_{15}(1688)$ for which one amplitude is too small by a factor of 2.

Hence, the purpose of this paper is twofold. Inelastic electron-proton scattering will be the first serious test of the relativistic version of the symmetric quark model. At the same time, if the $F_{15}(1688)$ photoproduction amplitude really is wrong by a factor of 2, this same disagreement should be seen in the electroproduction of this resonance. In addition, it is interesting to find out how well the interaction of longitudinally polarized photons which do not arise in photoproduction is described in this quark model.

In Sec. II we outline the kinematics relevant for the description of inelastic electron scattering in terms of amplitudes for internal excitations of the nucleon by the transverse and longitudinal parts of the virtual photon. These amplitudes are calculated in the relativistic quark model in Sec. III and the results obtained are discussed and compared with experiment in Sec. IV.

II. FORMALISM

We will assume that the inelastic electron-nucleon scattering process

$$e + N \to e' + N^* \tag{1}$$

proceeds through one-photon exchange as in Fig. 2. The initial and final electrons with four-momenta $k = (E; \vec{k})$ and $k' = (E'; \vec{k}')$ we take to be of zero mass. Then the invariant four-momentum transfer to the nucleon will be

$$q^2 = (k - k')^2 = -4EE' \sin^2(\tfrac{1}{2}\theta), \tag{2}$$

where θ is the electron scattering angle. In the lab system, the energy of the virtual photon with momentum $q = (\nu, \vec{Q})$ will be

$$\nu = E - E' = q \cdot p/m, \tag{3}$$

assuming the target nucleon to be at rest with mass m.

As shown by Bjorken and Walecka,[7] the differential cross section for this process can be written

$$\frac{d^2\sigma}{d\Omega dE'} = \frac{\alpha^2}{4E^2 \sin^4(\frac{1}{2}\theta)} \times [W_2(\nu, q^2)\cos^2(\tfrac{1}{2}\theta) + 2W_1(\nu, q^2)\sin^2(\tfrac{1}{2}\theta)] \tag{4}$$

assuming unpolarized initial and final nucleon states. The two invariant structure functions W_1 and W_2 are defined in terms of electromagnetic current matrix elements:

$$W_{\mu\nu} = 2m\left[\left(p_\mu - q_\mu \frac{p\cdot q}{q^2}\right)\left(p_\nu - q_\nu \frac{p\cdot q}{q^2}\right)\frac{W_2}{m^2} + \left(\frac{q_\mu q_\nu}{q^2} - g_{\mu\nu}\right)W_1\right] = \sum_n (2\pi)^3 \delta^4(p + q - p')\langle p|J_\mu(0)|n\rangle\langle n|J_\nu(0)|p\rangle, \tag{5}$$

where the sum extends over all final states $|n\rangle$ with four-momentum p'.

With only one nucleon resonance with mass M in the final state, $W_{\mu\nu}$ takes the form

$$W_{\mu\nu} = \langle p|J_\mu(0)|p'\rangle\langle p'|J_\nu(0)|p\rangle \delta(W^2 - M^2). \tag{6}$$

Here $W^2 = (p + q)^2$ is the invariant mass squared of the produced N^*.

The matrix elements

$$\langle p|J_\mu(0)|p'\rangle = 2Mf_\mu \tag{7}$$

must satisfy current conservation

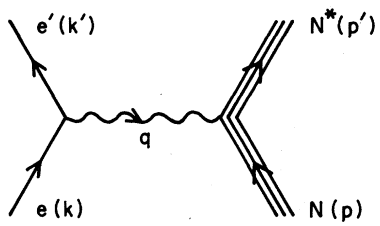

FIG. 2. One-photon exchange diagram for resonance electroproduction.

$$q_\mu \langle p|J_\mu(0)|p'\rangle = 0. \tag{8}$$

Going to the rest system of the N^*, where we take the space part of the photon four-momentum $q_\mu = (\nu^*, \vec{Q}^*)$ along the z axis, this requirement relates the scalar and longitudinal part of the current:

$$Q^* f_z = \nu^* f_t. \tag{9}$$

In this frame, following Bjorken and Walecka, we can now express W_1 and W_2 in terms of f_x, f_y, and f_t using Eq. (5):

$$W_1 = \frac{1}{2}(|f_x|^2 + |f_y|^2)\frac{M}{m}\delta(W-M),$$

$$W_2 = \frac{1}{2}\left(\frac{2q^4}{Q^{*4}}|f_t|^2 - \frac{q^2}{Q^{*2}}(|f_x|^2+|f_y|^2)\right)\frac{m}{M}\delta(W-M). \tag{10}$$

Defining partial cross sections due to the transverse and longitudinal parts of the photon by

$$\sigma_t(W) = \frac{4\pi^2\alpha}{Q^*}\frac{1}{2}(|f_x|^2+|f_y|^2)\delta(W-M),$$

$$\sigma_l(W) = \frac{4\pi^2\alpha}{Q^*}\left(\frac{+q^2}{Q^{*2}}\right)|f_t|^2\delta(W-M), \tag{11}$$

we can now write the differential cross section, Eq. (4), as

$$\frac{d^2\sigma}{d\Omega dE'} = \frac{\alpha}{4\pi^2}\frac{\cos^2(\frac{1}{2}\theta)}{4E^2\sin^4(\frac{1}{2}\theta)} \times\left(\frac{-q^2}{Q}\right)\frac{1}{\epsilon}(\sigma_t - \epsilon\sigma_l), \tag{12}$$

where

$$\epsilon^{-1} = 1 + 2\left(1-\frac{\nu^2}{q^2}\right)\tan^2(\tfrac{1}{2}\theta). \tag{13}$$

Instead of the cross sections σ_t and σ_l, experimental data are usually given for the slightly different quantities σ_T and σ_S introduced by Hand[8]:

$$\sigma_T = +\frac{Q}{K}\sigma_t, \quad \sigma_S = -\frac{Q}{K}\sigma_l. \tag{14}$$

Here K is the lab energy required to produce the N^* with real photons

$$K = (M^2 - m^2)/2m. \tag{15}$$

Inserting σ_T and σ_S into Eq. (12), we get the well-known expression

$$\frac{d^2\sigma}{d\Omega dE'} = \Gamma_T\sigma_T + \Gamma_S\sigma_S = \Gamma_T(\sigma_T + \epsilon\sigma_S), \tag{16}$$

with

$$\Gamma_T = \frac{\alpha}{4\pi^2}\left(\frac{-K}{q^2}\right)\frac{E'}{E}\frac{2}{1-\epsilon}. \tag{17}$$

The polarization parameter ϵ varies between 0 and 1.

From Eq. (11) we get for σ_T and σ_S:

$$\sigma_T(W) = \frac{4\pi^2\alpha}{K^*}\frac{1}{2}(|f_+|^2+|f_-|^2)\frac{\Gamma/2\pi}{(W-M)^2+\Gamma^2/4},$$

$$\sigma_S(W) = \frac{4\pi^2\alpha}{K^*}\left(\frac{-q^2}{Q^{*2}}\right)|f_0|^2\frac{\Gamma/2\pi}{(W-M)^2+\Gamma^2/4}, \tag{18}$$

where we have made the substitution

$$\delta(W-M) \to \frac{1}{\pi}\frac{\Gamma/2}{(W-M)^2+\Gamma^2/4} \tag{19}$$

valid for an unstable resonance having a total width Γ. K^* is the quantity K evaluated in the N^* rest frame

$$K^* = (M^2-m^2)/2M, \tag{20}$$

$$f_0 = f_t, \qquad f_\pm = \mp(\tfrac{1}{2})^{1/2}(f_x \pm i f_y), \tag{21}$$

so that f_+ and f_- correspond to photons with positive and negative helicity in the rest frame of N^* where the initial nucleon has $J_z = +\frac{1}{2}$.

In Sec. III we will calculate the matrix elements f_0, f_+, and f_- for all the relevant nucleon resonances in the symmetric quark model. Equation (18) can then be used to get the peak cross sections $\sigma_T(M)$ and $\sigma_S(M)$ which can be directly compared with experiment.

III. CURRENT MATRIX ELEMENTS

The relativistic symmetric quark model we will use here, as developed in Ref. 4, pictures the baryon as three quarks held together by pairwise harmonic forces. This system is described by the operator

$$K = 3(p_a^2 + p_b^2 + p_c^2) + \tfrac{1}{36}\Omega^2 \times[(u_a-u_b)^2 + (u_b-u_c)^2 + (u_c-u_a)^2] + C, \tag{22}$$

where p_a is the four-momentum of quark a with coordinate u_a. C is some unknown constant to describe the departure from this simple model. Introducing the total momentum P of the system and two internal momenta ξ and η,

$$p_a = \tfrac{1}{3}P - \tfrac{1}{3}\xi,$$

$$p_b = \tfrac{1}{3}P + \tfrac{1}{6}\xi - \frac{1}{2\sqrt{3}}\eta, \tag{23}$$

$$p_c = \tfrac{1}{3}P + \tfrac{1}{6}\xi + \frac{1}{2\sqrt{3}}\eta,$$

then Eq. (22) can be written

$$K = P^2 - \mathfrak{M}^2,$$

where

$$-\mathfrak{M}^2 = \tfrac{1}{2}(\xi^2+\eta^2) + \tfrac{1}{2}\Omega^2(x^2+y^2) + C. \tag{24}$$

Here x and y are coordinates conjugate to ξ and η. To discuss the mass spectrum following from this internal motion, it is more convenient to use the creation operators

$$a^\dagger = \left(\frac{1}{2\Omega}\right)^{1/2}\xi + i\left(\frac{\Omega}{2}\right)^{1/2}x,$$
$$b^\dagger = \left(\frac{1}{2\Omega}\right)^{1/2}\eta + i\left(\frac{\Omega}{2}\right)^{1/2}y, \tag{25}$$

and their Hermitian conjugates a and b. In terms of these, Eq. (24) takes the form

$$-\mathfrak{M}^2 = \Omega(a^\dagger a + b^\dagger b) + C. \tag{26}$$

The eigenvalues of this operator give an equally spaced spectrum in mass squared, each excitation corresponding to $\Omega = 1.05\ \mathrm{GeV}^2$.

In the symmetric quark model, every physical baryon state is required to be totally symmetric under any interchange of its quark labels. Consequently, each excited state must be combined with the appropriate SU(6) state to give over-all symmetry under combined interchange of both SU(6) and spatial quark labels. The lowest SU(6)⊗O(3) multiplets resulting from this restriction are listed in Table I together with their decomposition into $^{2S+1}(\mathrm{SU}(3))_J$ multiplets, S being the quark spin of the SU(3) multiplet and J the total angular momentum. Each multiplet is identified by one representative particle: the N in octets, the Δ in decimets, and the Λ in singlets. The multiplets with a question mark in front are not yet established, but they are predicted to exist. Their mass follows from the extra assumption of negligible spin-orbit forces.[9]

The electromagnetic interaction of the baryons is obtained in this model through the minimal coupling

$$p_\mu \to p_\mu - eA_\mu \tag{27}$$

for each quark four-momentum p_μ. As shown in Ref. 4, this gives for the coupling to a photon with polarization e_μ in the rest system of the N^*:

$$\begin{aligned}\Delta\mathfrak{M}^2 &= J_\mu A_\mu \\ &= 9Ge_a \exp\left[-\left(\frac{2}{\Omega}\right)^{1/2} q\cdot a^\dagger\right]\left[\left(\frac{2}{3}M - \frac{1}{3}\nu^* - \frac{Q^{*2}}{2mg^2}\right)e_t + \frac{2}{3}\left(\frac{\Omega}{2}\right)^{1/2}(\vec{a}^\dagger + \vec{a})\cdot\vec{e} + (\vec{Q}^*\cdot\vec{e})\left(\frac{1}{3} + \frac{\nu^*}{2mg^2}\right)\right. \\ &\quad \left. + i\vec{\sigma}_a\cdot(\vec{Q}^*\times\vec{e})\left(1 + \frac{\nu^*}{2mg^2}\right)\right]\exp\left[+\left(\frac{2}{\Omega}\right)^{1/2} q\cdot a\right].\end{aligned} \tag{28}$$

Here e_a and $\vec{\sigma}_a$ are the charge and spin of quark a and

$$g^2 = \frac{(M+m)^2 - q^2}{4Mm}. \tag{29}$$

$G = G(M, q^2)$ is an unknown form factor we will return to in Sec. IV.

Taking the photon momentum $\vec{Q}^*$ along the z axis and substituting for the photon energy

$$\nu^* = (M^2 - m^2 + q^2)/2M, \tag{30}$$

we get from Eq. (28) for the current matrix elements

$$\begin{aligned} f_0 &= 9G\langle N(+\tfrac{1}{2})|e_a S e^{-\lambda a_z}|N^*(+\tfrac{1}{2})\rangle, \\ f_- &= 9G\langle N(+\tfrac{1}{2})|e_a(Ta_+ + R\sigma_{a-})e^{-\lambda a_z}|N^*(+\tfrac{3}{2})\rangle, \\ f_+ &= 9G\langle N(+\tfrac{1}{2})|e_a(Ta_- + R\sigma_{a+})e^{-\lambda a_z}|N^*(-\tfrac{1}{2})\rangle, \end{aligned} \tag{31}$$

where

$$\begin{aligned} &\lambda = \left(\frac{2}{\Omega}\right)^{1/2} Q^*, \quad T = \frac{1}{3M}\left(\frac{\Omega}{2}\right)^{1/2}, \\ &S = +(3Mm + q^2 - m^2)/6M^2, \\ &R = \sqrt{2}\, Q^* \frac{M+m}{(M+m)^2 - q^2}, \end{aligned} \tag{32}$$

and

$$Q^{*2} = -q^2 + (M^2 - m^2 + q^2)^2/4M^2.$$

From Eq. (28) we find

$$f_t = cS, \tag{33}$$
$$(Q^*/\nu^*)f_z = cS - c(M^2 - m^2 - N\Omega)/6M\nu^*, \tag{34}$$

where c is some numerical constant and N is the number of excitations in the N^*.

In this model, all particles are on straight exchange-degenerate trajectories with masses $M^2 = m^2 + N\Omega$, m being the mass of the ground state. The last term in Eq. (34) will then be zero and the current conservation condition, Eq. (9), is satisfied.

To be consistent at this point, we should also use the model values of the particle masses in the numerical calculations of the scattering amplitudes. This would, however, bring us into trouble with the kinematical factors entering the cross-section formulas where we must use the physical masses of the particles involved. Consequently, we will in the following use the real particle masses in all expressions. In the cases considered, this makes little difference in the numerical

TABLE I. Lowest resonance multiplets in the symmetric quark model.

No. of excitations	Excitation	SU(6)⊗O(3)	$^{2S+1}(\mathrm{SU}(3))_J$	Resonance
$N=0$		$[\underline{56}, 0^+]$	$^2(\underline{8})_{1/2}$	$P_{11}(938)$
			$^4(\underline{10})_{3/2}$	$P_{33}(1236)$
$N=1$	$\vec{a}^\dagger, \vec{b}^\dagger$	$[\underline{70}, 1^-]$	$^2(\underline{1})_{1/2}$	$S_{01}(1405)$
			$^2(\underline{1})_{3/2}$	$D_{03}(1520)$
			$^2(\underline{8})_{1/2}$	$S_{11}(1535)$
			$^2(\underline{8})_{3/2}$	$D_{13}(1520)$
			$^4(\underline{8})_{1/2}$	$S_{11}(1700)$
			$^4(\underline{8})_{3/2}$	$?D_{13}(1700)$
			$^4(\underline{8})_{5/2}$	$D_{15}(1670)$
			$^2(\underline{10})_{1/2}$	$S_{31}(1650)$
			$^2(\underline{10})_{3/2}$	$D_{33}(1670)$
$N=2$	$\vec{a}^\dagger\cdot\vec{a}^\dagger+\vec{b}^\dagger\cdot\vec{b}^\dagger$	$[\underline{56}, 0^+]$	$^2(\underline{8})_{1/2}$	$P_{11}(1470)$
			$^4(\underline{10})_{3/2}$	$?P_{33}(1690)$
	$\vec{a}^\dagger\vec{a}^\dagger+\vec{b}^\dagger\vec{b}^\dagger$	$[\underline{56}, 2^+]$	$^2(\underline{8})_{3/2}$	$?P_{13}(1700)$
			$^2(\underline{8})_{5/2}$	$F_{15}(1688)$
			$^4(\underline{10})_{1/2}$	$P_{31}(1910)$
			$^4(\underline{10})_{3/2}$	$?P_{33}(1920)$
			$^4(\underline{10})_{5/2}$	$F_{35}(1890)$
			$^4(\underline{10})_{7/2}$	$F_{37}(1950)$
	$\vec{a}^\dagger\cdot\vec{a}^\dagger-\vec{b}^\dagger\cdot\vec{b}^\dagger$, $\vec{a}^\dagger\cdot\vec{b}^\dagger$	$[\underline{70}, 0^+]$	$^2(\underline{8})_{1/2}$	$P_{11}(1780)$
	$\vec{a}^\dagger\vec{a}^\dagger-\vec{b}^\dagger\vec{b}^\dagger$, $\vec{a}^\dagger\vec{b}^\dagger$	$[\underline{70}, 2^+]$	$^2(\underline{8})_{3/2}$	$P_{13}(1860)$
			$^4(\underline{8})_{7/2}$	$F_{17}(1990)$
	$\vec{a}^\dagger\times\vec{b}^\dagger$	$[\underline{20}, 1^+]$		

results of the model.

In particular, for the $F_{15}(1688)$ which is the Regge recurrence of the nucleon, one should expect the calculated amplitudes to be in the best agreement with experiment. As discussed in Sec. I, this is apparently not the case.

Using the Appendix in Ref. 4, it is a simple matter to evaluate the matrix elements in Eq. (31). The results are given in Table II where we have only included those resonances with mass $M<1750$ MeV, this being the region of interest here.

TABLE II. Helicity amplitudes for proton target with $J_z=+\frac{1}{2}$.

State	Γ (MeV)	f_-/G	f_+/G	f_0/G
$P_{33}(1236)$	120	$-\sqrt{6}\,R$	$+\sqrt{2}\,R$	0
$P_{11}(1470)$	250		$-(\frac{3}{4})^{1/2}R\lambda^2$	$-(\frac{3}{4})^{1/2}S\lambda^2$
$D_{13}(1520)$	120	$+(\frac{9}{2})^{1/2}T$	$+(\frac{3}{2})^{1/2}T-\sqrt{3}\,R\lambda$	$-\sqrt{3}\,S\lambda$
$S_{11}(1535)$	120		$-\sqrt{3}\,T-(\frac{3}{2})^{1/2}R\lambda$	$+(\frac{3}{2})^{1/2}S\lambda$
$S_{31}(1650)$	150		$-\sqrt{3}\,T+(\frac{1}{6})^{1/2}R\lambda$	$+(\frac{3}{2})^{1/2}S\lambda$
$D_{33}(1670)$	240	$+(\frac{9}{2})^{1/2}T$	$+(\frac{3}{2})^{1/2}T+(\frac{1}{3})^{1/2}R\lambda$	$-\sqrt{3}\,S\lambda$
$D_{15}(1670)$	140	0	0	0
$F_{15}(1688)$	125	$-(\frac{18}{5})^{1/2}T\lambda$	$[-(\frac{9}{5})^{1/2}T+(\frac{9}{10})^{1/2}R\lambda]\lambda$	$+(\frac{9}{10})^{1/2}S\lambda^2$
$?P_{33}(1690)$	?250	$+(\frac{1}{2})^{1/2}R\lambda^2$	$-(\frac{1}{6})^{1/2}R\lambda^2$	0
$S_{11}(1700)$	250		0	0
$?D_{13}(1700)$	?150	0	0	0
$?P_{13}(1700)$	?200	$+(\frac{9}{10})^{1/2}T\lambda$	$[+(\frac{27}{10})^{1/2}T+(\frac{3}{5})^{1/2}R\lambda]\lambda$	$-(\frac{3}{5})^{1/2}S\lambda^2$

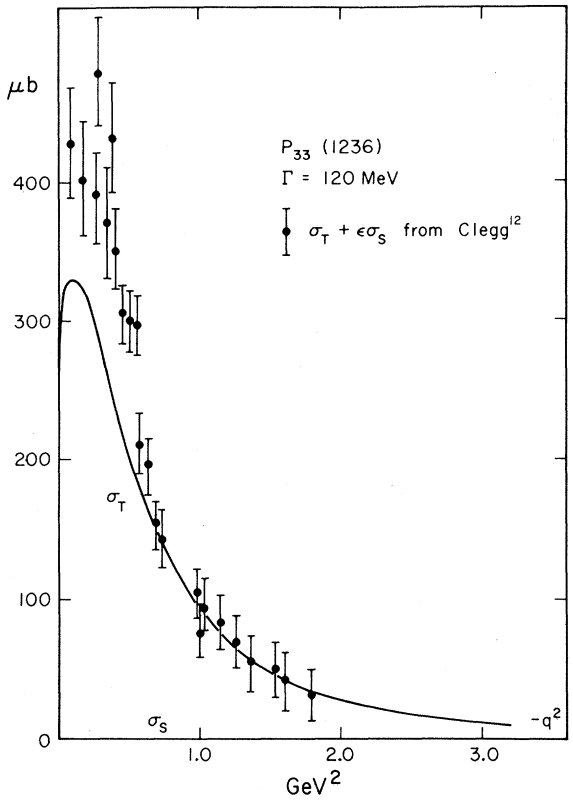

FIG. 3. Resonance cross section at $W = 1236$ MeV with proton target. Data from Ref. 12.

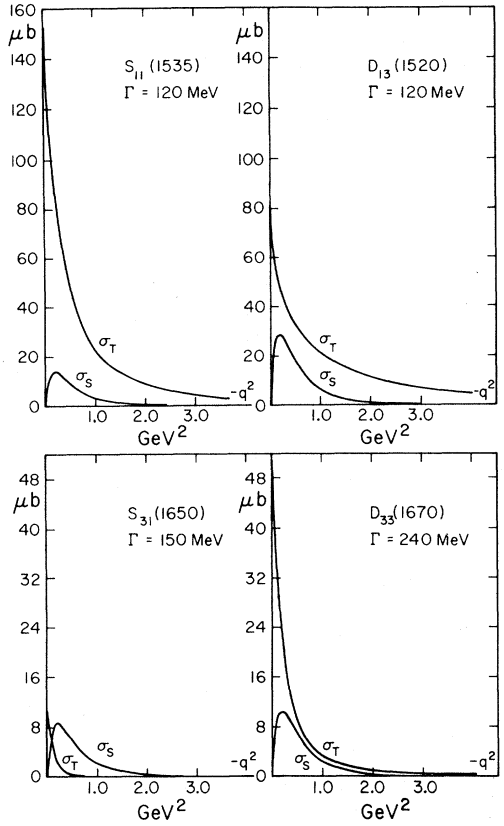

FIG. 4. Transverse (σ_T) and scalar (σ_S) cross sections for the $S_{11}(1535)$, $D_{13}(1520)$, $S_{31}(1650)$, and $D_{33}(1670)$ resonances with proton target.

IV. RESULTS AND DISCUSSION

The form factor G does not follow from this model as discussed in Ref. 4. Our lack of theoretical understanding at this point forces us to guess its form and see how that guess compares with experiment. We have one serious restriction on our choice. It should, in the simple case of elastic electron scattering, give the proton dipole form factor. With this in mind, we will in the following use one of the simplest possible forms:

$$G(M, q^2)=\left(1-\frac{q^2}{0.71}\right)^{-2}\left(1-\frac{q^2}{4M^2}\right)^{(1-N)/2}, \quad (35)$$

where N is the number of excitations in the N^*. This arbitrary choice seems to give a reasonable description of the present experimental data in the limited resonance region we are concerned with here. From Eq. (50) in Ref. 4, we get for the proton magnetic form factor with this assumed form, Eq. (35):

$$\frac{G_M}{\mu}=\left(1-\frac{q^2}{0.71}\right)^{-2}. \quad (36)$$

We are now in the position to calculate the cross sections σ_T and σ_S, Eq. (18), for each state in Table II. The results of the numerical work are presented in Figs. 3, 4, and 5 where we plot each cross section for proton target at the resonance peak $W = M$ as a function of $-q^2$.

The scalar cross section for the $P_{33}(1236)$ is zero since this resonance has quark spin $S=\frac{3}{2}$. Both σ_T and σ_S vanish for all the three states $S_{11}(1700)$, $D_{13}(1700)$, and $D_{15}(1670)$ of the quark spin $S=\frac{3}{2}$ octets of the $[\underline{70}, 1^-]$. The reason is that the electromagnetic coupling between two octet protons being proportional to $F+\frac{1}{3}D$ vanishes for these states since they all have $F/D=-\frac{1}{3}$.

In Fig. 5 we have also included cross sections for the $P_{33}(1690)$, existing in the footnotes of the Particle Tables,[10] and the not-yet-established $P_{13}(1700)$ with an assumed width of $\Gamma = 200$ MeV just to find out how important the contributions from these resonances are.

From Fig. 1 we see that there are three prominent bumps in the inelastic electron-proton cross section. The dominant peak is at $W = 1236$ MeV, corresponding to the $P_{33}(1236)$ resonance. The next bump is at $W = 1525$ MeV and the last at $W = 1680$ MeV. There is also some structure

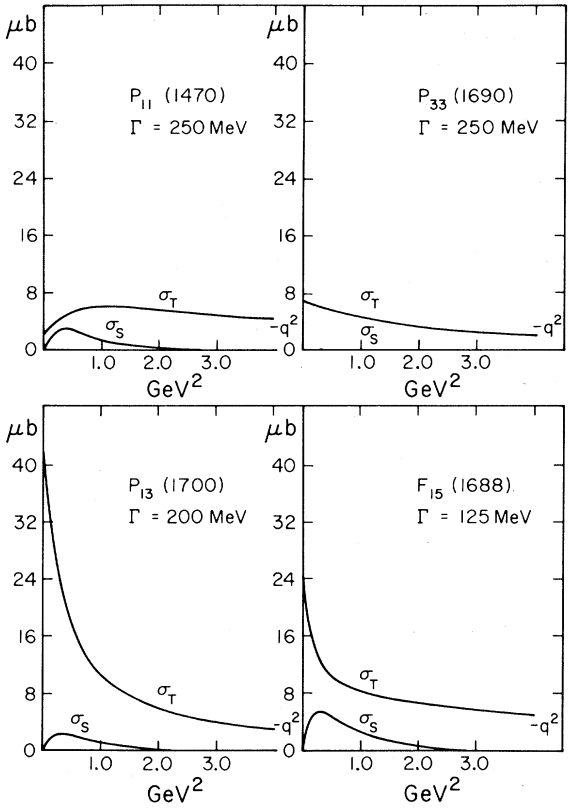

FIG. 5. Transverse (σ_T) and scalar (σ_S) cross sections for the $P_{11}(1470)$, $P_{33}(1690)$, $P_{13}(1700)$, and $F_{15}(1688)$ resonances with proton target.

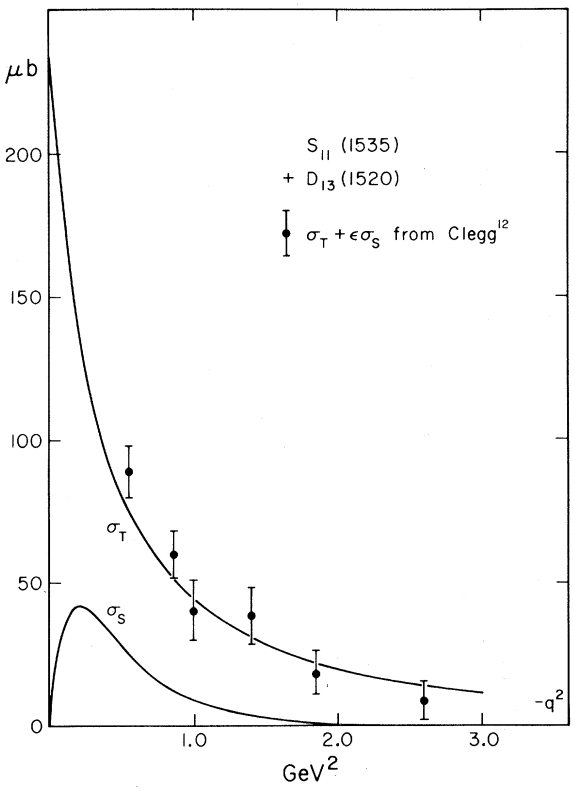

FIG. 6. Total transverse (σ_T) and scalar (σ_S) cross sections at the second resonance peak $W = 1525$ MeV with proton target. Data from Ref. 12.

around $W = 1920$ MeV which we will not discuss here because of its dubious resonance nature.[11] The second and third peaks can be qualitatively understood in terms of the resonances in Table II. Besides the $P_{33}(1236)$ and the Roper resonance $P_{11}(1470)$ which has a small cross section, the resonances are grouped into two distinct mass regions. The first group consists of the $S_{11}(1535)$ and the $D_{13}(1520)$ corresponding to the second bump. The remaining resonances, grouped around $W = 1680$ MeV, are the $S_{31}(1650)$, $D_{15}(1670)$, $D_{33}(1670)$, $F_{15}(1688)$, $P_{33}(1690)$, $S_{11}(1700)$, $D_{13}(1700)$, and $P_{13}(1700)$.

To make a quantitative comparison with experiment, we have in Fig. 3 for the $P_{33}(1236)$ plotted the experimental values of $\Sigma = \sigma_T + \epsilon\sigma_S$ as evaluated by Clegg.[12] For $-q^2 < 0.5$ GeV^2, we see that the theoretical cross section is almost 30% too small. For larger $-q^2$, the agreement is very good. The values of Σ at the second resonance peak we compare with the sum of the cross sections of $S_{11}(1535)$ and $D_{13}(1520)$ in Fig. 6. Again we find very good agreement. At small $-q^2$, the largest contribution is coming from the $S_{11}(1535)$, contrary to what is usually assumed in the literature.[11,12]

Doing the same for the third peak, Fig. 7, we note that good agreement is obtained only when including the predicted resonance $P_{13}(1700)$. Without its contribution we would get a cross section around 30% too small compared with the experimental data of Clegg.[12]

It is generally believed that this third bump in the cross section is mainly $F_{15}(1688)$.[11,12] According to the present model, that is not the case, the $D_{33}(1670)$ being just as important. Had we tried to use the $F_{15}(1688)$ alone, we would be off by a factor of 3 in the cross section. This may explain the apparent disagreement for this resonance in the photoproduction amplitude which experimentally is found by fits not including all the important resonances in the same mass region like the $D_{33}(1670)$.[13]

In other words, had the $F_{15}(1688)$ alone been able to explain the third peak, then this model would be in serious trouble. The same would obviously have been the case if we had gotten good agreement not taking into account the not-yet-observed $P_{13}(1700)$.

Another interesting result of this model is the small scalar cross section σ_S we find. The maximum of the ratio σ_S/σ_T reached at $-q^2 \simeq 0.5$ GeV^2

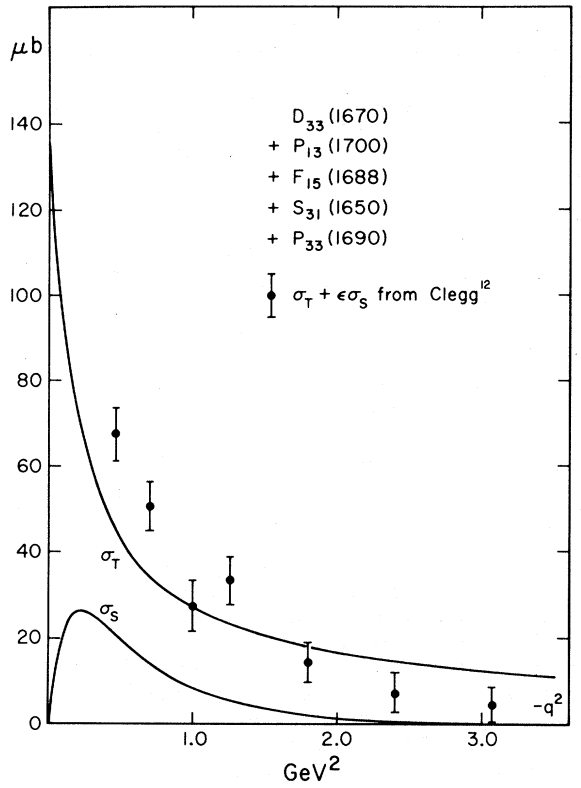

FIG. 7. Total transverse (σ_T) and scalar (σ_S) cross sections at the third resonance peak $W=1680$ MeV with proton target. Data from Ref. 12.

is 30% at the second peak and near 50% at the third peak. It is substantially smaller for all other values of $-q^2$. This agrees nicely with recent experimental results from DESY[14] where the same ratio is found to be around 20% in the resonance region.

The reason for this small scalar cross section is easily found by looking at Eqs. (18) and (32). In addition to the required zero of σ_S at $q^2=0$, we see that $S=0$ at

$$-q^2 = m(3M - m) \tag{37}$$

so σ_S will also have a zero in the resonance region in the range $-q^2=3-4$ GeV^2. This result is obviously independent of the arbitrary form factor we have used.

A completely different approach to the process of electroproduction of nucleon resonances has been taken by Pritchett, Walecka, and Zucker[15] and Pritchett and Zucker.[16] They have used a coupled-channel relativistic N/D model to calculate the excitation amplitudes for most of the resonances considered in this paper. The magnitudes of the first three resonance peaks in the cross section obtained in this model agree fairly well with experiment. However, it also predicts that the scalar cross section should dominate at the second peak beyond $-q^2=4$ GeV^2 and at the third peak when $-q^2>1$ GeV^2. The new measurements of σ_S in this resonance region[14] seem to be in disagreement with these predictions.

V. CONCLUSION

The resonance region of inelastic electron-proton scattering has been investigated in a relativistic quark model. We have found good agreement with all aspects of the present experimental situation. The second peak in the inelastic cross section is well described by the resonances $S_{11}(1535)$ and $D_{13}(1520)$. To obtain good agreement for the third peak, we need to include, besides the $F_{15}(1688)$, the $D_{33}(1670)$ and a not-yet-observed resonance $P_{13}(1700)$ whose existence is predicted from this symmetric quark model. We find a small cross section for the Roper resonance $P_{11}(1470)$ which is also in accordance with experiment. The scalar cross section σ_S is smaller than σ_T in the whole resonance region considered.

We look forward to more precise experiments for small $-q^2$ which would test our choice of form factor. Future coincidence experiments will be important to check the composition of each bump of the inelastic cross section.

---

*Work supported in part by the U. S. Atomic Energy Commission under Contract No. AT(11-1)-68.

[1]R. E. Taylor, in *Proceedings of the Fifteenth International Conference on High Energy Physics, Kiev, U.S.S.R., 1970* (Atomizdat, Moscow, to be published), and references quoted therein.

[2]M. Gell-Mann, Phys. Letters 8, 714 (1964); G. Zweig, CERN Report No. CERN-TH-401 (unpublished); CERN Report No. CERN-TH-412 (unpublished).

[3]N. S. Thornber, Phys. Rev. 169, 1096 (1968); N. S. Thornber, Phys. Rev. D 3, 787 (1971).

[4]R. P. Feynman, M. Kislinger, and F. Ravndal, Phys. Rev. D 3, 2706 (1971). The metric used is such that for a four-momentum $p_\mu=(E,\vec{p})$, $p^2=p_\mu p_\mu=E^2-\vec{p}^2=m^2$. The states $|p\rangle$ have the invariant normalization $\langle p'|p\rangle=(2\pi)^3 2E\delta^3(\vec{p}-\vec{p}')$ and $\bar{u}u=2m$.

[5]D. Faiman and A. W. Hendry, Phys. Rev. 180, 1572 (1969); L. A. Copley, G. Karl, and E. Obryk, Phys. Letters 29B, 117 (1969).

[6]R. L. Walker, in *International Symposium on Electron and Photon Interactions at High Energies, Liverpool, England, 1969*, edited by D. W. Braben and R. E. Rand (Daresbury Nuclear Physics Laboratory, Daresbury, Lancashire, England, 1970).

[7]J. D. Bjorken and J. D. Walecka, Ann. Phys. (N.Y.) 38, 35 (1966).

[8]L. N. Hand, Phys. Rev. 129, 1834 (1963).
[9]R. P. Feynman, S. Pakvasa, and S. F. Tuan, Phys. Rev. D 2, 1267 (1970).
[10]Review of Particle Properties, Particle Data Group Phys. Letters 33B, 1 (1970).
[11]M. Breidenbach, MIT Report No. MIT-2098-635, 1970 (unpublished).
[12]A. B. Clegg, Ref. 6.
[13]R. L. Walker, private communication.
[14]F. W. Brasse *et al.*, DESY Report No. 71/2, 1971 (unpublished).
[15]P. L. Pritchett, J. D. Walecka, and P. A. Zucker, Phys. Rev. 184, 1825 (1969).
[16]P. L. Pritchett and P. A. Zucker, Phys. Rev. D 1, 175 (1970).

PHYSICAL REVIEW D VOLUME 4, NUMBER 5 1 SEPTEMBER 1971

Two-Body Weak Reactions of Hadrons at Very High Energies*

Mark Dubovoy, Paul Langacker,† and Mahiko Suzuki
Department of Physics and Lawrence Radiation Laboratory, University of California, Berkeley, California 94720
(Received 2 April 1971)

Two-body hadronic scattering through weak interactions is investigated theoretically in the energy region accessible at the National Accelerator Laboratory. In the ordinary current ×current form of weak interactions, the following quantities are calculated for charge-exchange weak hadronic reactions: (i) the differential cross section, the polarization of a final baryon, and the asymmetry in the angular distribution of scattering from a polarized target for strangeness-changing processes, and (ii) the interference of weak-interaction amplitudes with strong-interaction amplitudes for processes to which both weak and strong interactions contribute. The interference with strong amplitudes is discussed by means of a straight extrapolation of existing Regge analysis at lower energies (less than 30 GeV). Differential cross sections near the forward direction are typically of the order of 10^{-38} cm^2 in $d\sigma/d\cos\theta$ in the center-of-mass frame. The interference between weak and strong amplitudes is unfortunately only one part in 10^4–10^5 for the πN charge-exchange scattering in spite of the different high-energy behavior. All calculations are supposed to be valid at high energies up to absorption corrections due to a Regge cut generated by the Pomeranchukon and a fixed pole at $J=1$ from the weak amplitude. Inelastic scattering is also briefly mentioned. Charge-nonexchange processes are discussed in connection with a test for the existence of neutral weak currents.

I. INTRODUCTION

The structure of weak interactions is fairly well known in the low-momentum-transfer region through semileptonic and purely leptonic decay processes.[1] In contrast, purely hadronic weak interactions are less understood, partly because of complications caused by strong interactions. For instance, neutral weak currents have frequently been discussed in connection with the $\Delta I=\frac{1}{2}$ rule, CP violation, and so forth; while their absence is now established to a very good accuracy in semileptonic and leptonic interactions, little can be said about purely hadronic processes.

A cutoff momentum characteristic of weak interactions has been extensively discussed from various viewpoints, recently by means of current algebras.[2-4] Some current-algebra calculations indicate a surprisingly low value of the cutoff momentum as compared with a unitarity cutoff (~300 GeV), although they are partly based on a somewhat controversial technique. It is very interesting to see how our weak-interaction theory, which has successfully described low-energy decay phenomena aside from CP-violating phenomena, must be modified at a short distance. Reactions induced by neutrinos have been thoroughly discussed,[5] since one can develop fairly straightforward arguments similar to those used for electroproduction as measured at SLAC. However, purely hadronic interactions have seldom been considered seriously. The purpose of this paper is to report results of our calculation of various quantities which may possibly be measured in future experiments on purely hadronic weak interactions at high energies.

We shall first consider two-body reactions. The current×current theory of weak interactions gives rise to a fixed pole at $J=1$ in the t-channel complex angular momentum plane.[6] The fixed pole appears in the t channels for reactions with $I=1$, $S=0$, and $|Q|=1$ and with $I=\frac{1}{2}$, $|S|=1$, and $|Q|=1$. We shall not take into account higher orders of